文章编号:1671-1637(2012)03-0037-07

货运机车车钩缓冲装置动力学仿真模型

吴 庆[1],罗世辉[1],魏冲锋[2],马卫华[1]
(1. 西南交通大学 牵引动力国家重点实验室,四川 成都 610031;
2. 伯明翰大学 机械工程学院,西米德兰兹 伯明翰 B152TT)

摘 要:分析了不同钩缓装置的工作原理,采用控制系统仿真方法建立了考虑实时性对中钩肩与钩尾摩擦副作用的钩缓装置结构模型,采用函数查表法建立了具有迟滞特性的非线性缓冲器模型,采用由 2 台 8 轴机车及 1 辆简化货车组成的列车模型对 DFC-E100 与 13A/QKX-100 钩缓装置进行了仿真研究,同时对车体稳钩能力进行了理论计算。计算结果表明:钩缓装置模型能够较好地反映机车钩缓装置的实际运行状态,DFC-E100 钩缓装置车钩在纵向力超过一定值后才会发生明显偏转,钩肩结构能够有效地防止车钩的过度偏转;机车配备 DFC-E100 钩缓系统时车体稳钩能力的仿真结果及理论计算结果与实测结果的误差分别为 4.23%和 10.65%。13A/QKX-100 系统车钩钩尾摩擦副是影响其承压行为的关键因素,其能使车钩在承受纵向压力时不发生明显偏转。

关键词:铁道车辆;货运机车;钩缓装置;仿真模型;动态特性
中图分类号:U260.34 **文献标志码**:A

Dynamics simulation models of coupler systems for freight locomotive

WU Qing[1], LUO Shi-hui[1], WEI Chong-feng[2], MA Wei-hua[1]
(1. Traction Power State Key Laboratory, Southwest Jiaotong University, Chengdu 610031, Sichuan, China;
2. School of Mechanical Engineering, University of Birmingham, Birmingham B152TT, West Midlands, UK)

Abstract: The working principles of two types of coupler systems were analysed. Based on considering the friction pairs of coupler tails and real-time aligning shoulders, coupler system models were set up by using control system simulation method. Nonlinear draft gear with hysteresis characteristic was modelled by using table lookup method. DFC-E100 system and 13A/QKX-100 system were simulated in a train model consisting of two 8-axle locomotives and one simplified wagon. The theoretical calculation of carbody-stabilizing-coupler ability was performed. Calculation result indicates that the models can rationally reflect the dynamic behaviour of freight locomotive's coupler systems. The distinct angling behaviour of DFC-E100 system is only observed when buff forces are larger than a certain value, but the aligning shoulder of DFC-E100 system can effectively prevent coupler from excessive angling. The error of carbody-stabilizing-coupler ability between simulation value and field test value is 4.23%, and the error between theoretical calculation value and field test value is 10.65%. The friction pair of 13A/QKX100 system is key element in the control of coupler dynamic behaviour, and can prevent coupler from distinct angling under buff condition. 1 tab, 11 figs, 15 refs.

Receipt Date: 2011-11-22
Research Projects: National Natural Science Foundation of China (50775191, 51005190)
Author Resume: WU Qing(1987-), Male, Nanchong, Sichuan, Doctoral Student of Southwest Jiaotong University, Research on Vehicle System Dynamics, +86-28-87601973, wuqing1943@126.com.
Tutor Resume: LUO Shi-hui(1964-), Male, Ganzhou, Jiangxi, Professor of Southwest Jiaotong University, PhD, +86-28-86466203, shluo@swjtu.cn.

Key words: railway vehicle; freight locomotive; coupler system; simulation model; dynamic characteristic

0 Introduction

As an important part in trains, coupler system has tremendous influence on train dynamics performance by its dynamic behaviour[1-2]. The issue is more prominent in long heavy haul trains. Three derailment instances have happened to heavy haul locomotives on the Daqin Coal Line (China) in 10 000-ton class train traction and braking experiments. Investigation results indicate a direct involvement of coupler systems in these accidents[3]. Similar accidents have also occurred in other countries[4-5]. Because field test has high costs, coordination difficulties and certain risks, simulation study has become optimum choice to predict the dynamic behaviour of coupler system.

However, the studies of coupler dynamics are usually conducted within longitudinal dynamics, in which carbody is generally simplified to a rigid body with single longitudinal freedom, and the influence of detailed coupler structure is negligible[6-7]. In coupler angling behaviour simulator (CABS)[8] developed by Association of American Railroads (AAR), two coupling couplers are simplified to a rigid rod. Based on integrating coupler moment and draft gear characteristics, CABS can be used to calculate coupler angles and coupler forces under different conditions. One of the disadvantages of CABS lies in the simplification of vehicle models, which makes researchers have to resort to another commercial software package NUCARS to evaluate the influence of coupler angles and coupler forces on vehicle dynamics performance. In 2004, Shen et al proposed using various force elements to replace coupler systems' lateral, longitudinal and vertical characteristics[9]. The model can rationally reflect the force characteristics between vehicles, but the influences of coupler angling behaviour and other system structures are not considered. In 2008, In order to analyse locomotive derailments in experiments[3], Luo et al developed a model that incorporates free-angle characteristics, independent aligning shoulder and draft gear impedance characteristics[10-11]. The model can reflect the influence of coupler free-angle and aligning shoulder characteristics on locomotive dynamics performance, but its refinements are not enough and the hysteresis characteristics of draft gear, friction pair and the real-time characteristics of aligning shoulder that have significant influence on the dynamic behaviour of coupler system are not considered.

Based on the model in references[10-11], this paper proposes several refinements of coupler models by incorporating nonlinear hysteresis draft gear, real-time aligning shoulder and friction pair at coupler tails. Two detailed typical coupler system models are presented and their dynamic characteristics under different buff conditions are studied in train system. Nonlinear wheel-rail interface and track irregularity are incorporated into the simulation models.

1 Coupler systems of freight locomotives

Locomotives can be categorized into electric locomotives and diesel locomotives. Active freight diesel locomotives in China mainly include ND_5, DF_4, DF_8, HX_N3 and HX_N5, and active freight electric locomotives include 8K, SS_3, SS_4, HX_D1, HX_D2 and HX_D3. ND_5, HX_N3 and HX_N5 mainly adopt 102 coupler system (AAR SBE4936AE coupler along with NC390 draft gear), HX_D2 mainly adopts DFC-E100 coupler system (derived from Les Appareils Ferroviaires (LAF) 1785 coupler system), and the rest mainly are equipped with domestic No. 13 or 13A coupler but with various draft gears. For example, DF_8 adopts MX-1 friction type rubber draft gear, SS_3 adopts MT-2 friction type spring draft gear, and HX_D1 and HX_D3 adopt QKX-100 resilient rubber draft gear. Since DFC-E100 system and 13A/QKX-100 system

are most typical in China, the following studies will focus on the two systems.

Fig. 1 shows the structure of a DFC-E100 system. It's a round-pin system that utilizes yoke pin to provide a physical connection between coupler and yoke. DFC-E100 system has free angle of 3.5°-4.0° and the maximum structural angle of 19.0°. The type of system relates draft gear forces with coupler aligning forces via the bumps on its front followers. As a result, draft gear forces can be transformed into coupler aligning forces.

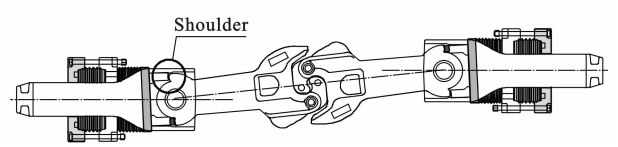

Fig. 1 DFC-E100 system

A 13A/QKX-100 system is illustrated in Fig. 2. It adopts draft keys rather than yoke pins to provide connection between couplers and yokes. Compared with DFC-E100 system, 13A/QKX-100 system has a larger free angle (9°-11°) and different approaches to confine coupler angling. Taking advantage of the special profile of draft key slot on yoke, the keys and the slots make up stops to stop coupler angling further when they reach the free angle. Another unique point of 13A/QKX-100 system is that each system has a pair of friction arc surfaces (radius is about 130 mm) between its coupler tail and front follower. Under buff force conditions, the friction pair can facilitate coupler with a strong dynamic stability.

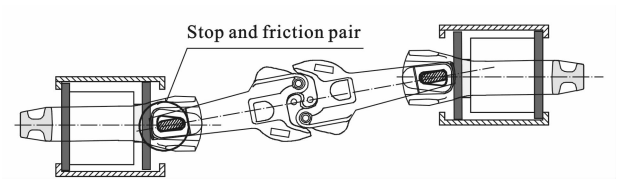

Fig. 2 13A/QKX-100 system

2 Draft gear models

Draft gear modelling has undergone a development from linear to nonlinear. The state of the art in draft gear modelling is demonstrated by nonlinear models with hysteresis characteristics[12-14]. In this paper, the table lookup method is utilized to model the nonlinear hysteresis characteristics of draft gear.

The hysteresis characteristics of draft gear mean the dissimilarity between its loading process and unloading process. The envelop area of loading curve and unloading curve indicates the energy that is absorbed within an operating cycle. The loading characteristics and unloading characteristics of draft gear can be defined as two functions of travel: $u(x)$ and $l(x)$, integrated with coupler gap, preload, rigid impact and some other features. Besides, a shift velocity e be defined. Therefore, when the current travel is x, the hysteresis force h can be expressed as

$$h=\begin{cases}|u(x)-l(x)| & |\Delta v|\geqslant e\\ |u(x)-l(x)|\dfrac{|\Delta v|}{e} & |\Delta v|<e\end{cases}\tag{1}$$

where Δv is the relative velocity of coupled carbodies. Because hysteresis force is alway opposite to the relative velocity, after introducing the sign function $\mathrm{sgn}(\Delta v)$, a draft gear model can be expressed as

$$F=\begin{cases}g(x)+|u(x)-l(x)|\mathrm{sgn}(\Delta v) & |\Delta v|\geqslant e\\ g(x)+|u(x)-l(x)|\mathrm{sgn}(\Delta v)\dfrac{|\Delta v|}{e} & |\Delta v|<e\end{cases}\tag{2}$$

where F is draft gear force; $g(x)$ is the impedance characteristic of draft gear, and should be replaced by $l(x)$ or $u(x)$ depending on working conditions. The model of draft gear is generalized in Fig. 3.

The response curves of a QKX-100 draft gear model and a DFC-E100 draft gear model are shown in Fig. 4. In this scenario, a mass of 100 t is

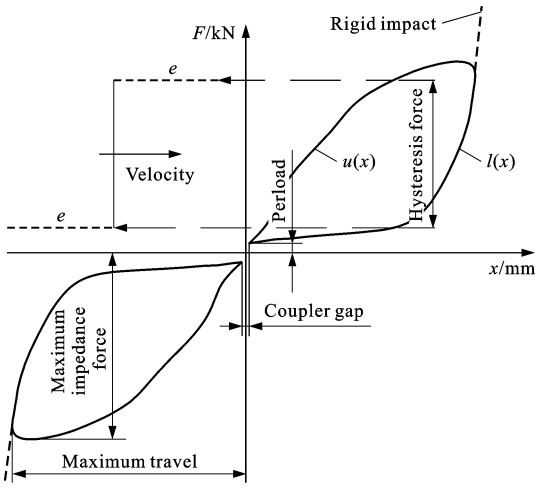

Fig. 3 Generalized model of draft gear

running into a stop at the speed of 9 km · h^{-1}. In Fig. 4, coupler gap, preload, resilient rubber draft gear characteristics, rigid impact, and other features are clearly demonstrated.

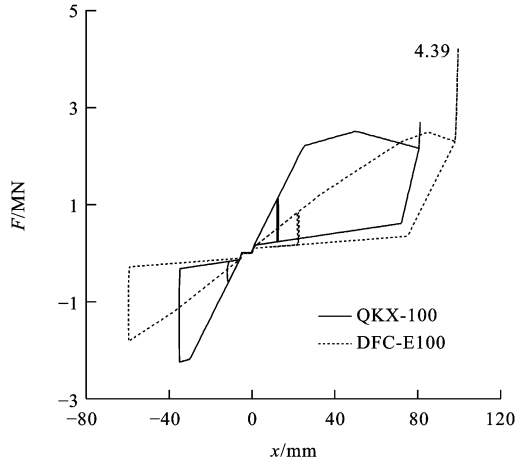

Fig. 4 Draft gear models

3 Coupler system models

A schematic of coupler models is illustrated in Fig. 5. Because coupler gap is incorporated in draft gear models, the two coupling couplers are simplified to a rigid rod. The modelling of yokes is neglected since both buff and draft characteristics are modelled in draft gear models. Couplers are assumed to be connected to followers directly and have a freedom of rotation about Z axis at point A. Followers are connected to carbodies by draft gear and have a freedom of transition along X axis. The longitudinal and lateral freedoms of couplers are constrained at point B. Integrating the vertical motion characteristics along with aligning shoulders (or stops) at points A and B, a detailed coupler model can be developed. With regard to the 13A coupler, friction pair must fulfill the model.

3.1 Aligning shoulder and stop characteristics

The aligning forces of DFC-E100 system are provided by the restoring forces of draft gear, and can be transformed into aligning torques. Both coupler free angle and structural maximum angle should be considered when modelling aligning shoulders, because in reality the rigid contact between coupler shanks and yokes will happen after coupler angle reaches the maximum angle. In order to improve the discontinuity in rigid contact modelling, the rigid contact is replaced by a large torsional stiffness, after which aligning shoulder characteristics can be expressed as

$$T=\begin{cases}0 & |\theta|<\alpha \\ FL\mathrm{sgn}(\theta) & \alpha\leqslant|\theta|\leqslant\beta \\ 10^8[\theta-\beta\mathrm{sgn}(\theta)]L & \beta<|\theta|\end{cases} \tag{3}$$

where T is aligning torque; θ is current coupler angle; α, β are coupler free angle and structural maximum angle respectively; L is the distance from aligning shoulder contact point to yoke pin center, it also indicates the effective arm of aligning torque.

With regard to the 13A/QKX100 system, the rigid contact between draft keys and draft key slots (on yokes) will happen when coupler angle reaches free angle. The modelling method of rigid contact used in the modelling of aligning shoulder can also be used in the modelling of stop, and its property is

$$T=\begin{cases}0 & |\theta|<\alpha \\ 10^8[\theta-\alpha\mathrm{sgn}(\theta)]L & |\theta|\geqslant\alpha\end{cases} \tag{4}$$

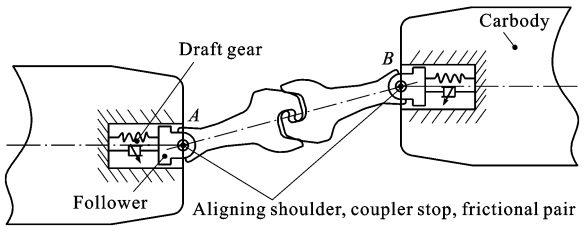

Fig. 5 Coupler model

3.2 Friction pair models

Because draft gear forces are used to indicate coupler forces, and are also used as the inputs of friction nominal forces. Only when couplers are bearing buff forces, friction pair will work. For $F>0$ (buff force)

$$f=\begin{cases}0 & |v_r|=0 \\ \dfrac{v_r}{v_f}F\mu & |v_r|<v_f \\ F\mu\,\mathrm{sgn}(v_r) & |v_r|\geqslant v_f\end{cases} \tag{5}$$

For $F\leqslant 0$ (draft force)

$$f=0 \tag{6}$$

where f is friction force; v_r is relative velocity of contact point; v_f is kinetic friction velocity; μ is friction coefficient.

4 Dynamics simulation

Referring to the structural parameters of a real 8-axle locomotive, two 8-axle heavy haul electric freight locomotive models are accomplished and used to form train models with DFC-E100 or 13A/QKX-100 system. In Fig. 6 a train simulation model consists of four detailed locomotives and one simplified freight wagon in head-end configuration. The configuration is selected as it exists in reality and can provide the largest load for locomotive couplers when train is hauling or braking. The simplified freight wagon model with a mass of 20 000 t has a single longitudinal freedom. Some of key parameters used in the models are listed in Tab. 1.

Tab. 1 Key parameters of train models

Parameter	Value	Parameter	Value
Preload(DFC/QKX)/kN	130/150	Aligning torque arm(DFC)/mm	135
Maximum travel(DFC/QKX)/mm	110/83	Kinetic friction velocity/(m·s^{-1})	0.02
Absorptivity (DFC/QKX)/%	80/70	Friction coefficient	0.32
Maximum impedance force/kN	2 500	Wheelbase/mm	2 600
Shift velocity/(m·s^{-1})	0.1	Bogiebase B'/mm	10 800
Coupler free angle (DFC/QKX)/(°)	3.5/9.0	Couplerbase C/mm	15 652
Coupler gap/mm	10	Lateral gap of secondary stop δ/mm	60
Coupler length G/mm	830	Lateral stiffness of primary suspension k_1/(kN·mm^{-1})	7.24
Coupler structural maximum angle (DFC)/(°)	19	Lateral stiffness of secondary suspension k_2/(kN·mm^{-1})	0.26

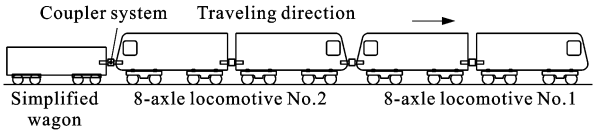

Fig. 6 Train model

The simulated scenario is dynamic braking, and the dynamic behaviour of the fourth coupler system bearing the largest longitudinal force is paid attention. Trains are running at a speed of 60 km·h^{-1} on a straight track without any gradient. Track irregularity standard AAR5 is selected. Locomotive brakes at the 2nd s, the braking force reaches its maximum value (75 kN per axle) at the 12th s, and the value is maintained until the simulation terminates.

5 Simulation result analysis

5.1 DFC-E100 system

The time histories of coupler force and coupler angle of a DFC-E100 system are given in Fig. 7. Under bearing a longitudinal buff force of 1 200 kN, the coupler of DFC-E100 system angles obviously. But coupler angle is effectively confined at the neighbourhood of free angle 3.5°. Coupler distinctly angles when coupler force increases to a certain value rather than at the starting point. Besides, obvious coupler force oscillations are detected when the large coupler angling occurs. The phenomenon is also observed in heavy haul field experiments[15].

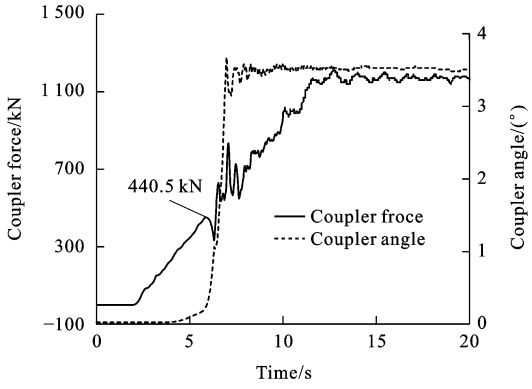

Fig. 7 Dynamic performances of DFC-E100 system

Under the joint effects of suspensions (both the primary and secondary suspensions) and carbody structures, locomotive carbodies have certain coupler-stabilizing ability. In other words, without any assistance from coupler-stabilized structures (friction pairs, stops or aligning shoulders), carbodies can prevent couplers from large angling under a certain longitudinal buff force. The stability is termed as carbody-stabilizing-coupler

ability, its reference point is the lowest longitudinal buff force, at which couplers and carbodies can not restore to their initial positions. The value also can be obtained through theoretical analysis in Fig. 8. In Fig. 8: F_a and F_b are coupler lateral forces; K is equivalent lateral stuffiness per bogie; φ is carbody yaw angle; F_c is coupler force.

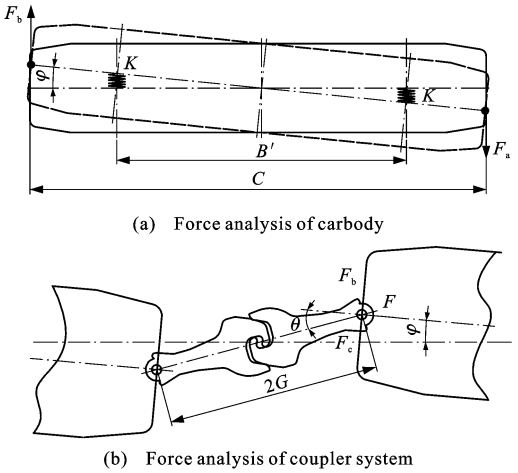

Fig. 8 Analysis of carbody-stabilizing-coupler ability

Based on the geometry relation in Fig. 8, the equation of carbody-stabilizing-coupler ability can be derived by the force-balance principle and the torque-balance principle

$$F = \frac{2K\delta B'}{C(1+k)} \frac{\cos(\varphi) - \sin(\varphi)\tan(\theta-\varphi)}{\sin(\theta) + \cos(\varphi)\tan(\theta-\varphi)} \quad (7)$$

$$k = \frac{|F_a|}{|F_b|} \quad (8)$$

With the same coupler angle, the value of k is equal to the absolute value of carbody's front-end longitudinal force to rear-end longitudinal force. The value of k in this paper is 0.75. Due to the confinements of secondary suspension stops, the yaw angle of carbody meets

$$\varphi = \frac{\delta}{1/2B'} \quad (9)$$

According to the geometrical relations between carbodies and couplers, current coupler angle can be expressed as

$$\theta = \arcsin\left(\frac{C\delta}{B'G}\right) + \varphi \quad (10)$$

If the values of θ and φ are small, Eq. 7 can be transformed into

$$F = \frac{2K\delta B'}{C(1+k)} \frac{B'G - 2\delta^2 C}{B'(\delta C + 2\delta G)} \quad (11)$$

Each bogie in the simulated locomotives has 4 primary suspension units and 4 secondary suspension units. Their connection modes are: all primary suspension units and all secondary suspension units are parallelly connected respectively; the primary suspension units are connected in series with the secondary suspension units. So the equivalent lateral stuffiness per bogie is

$$K = \frac{4k_1k_2}{k_1+k_2} \quad (12)$$

It is seen from Eq. 11 that carbody-stabilizing-coupler stability is relevant to locomotive structures, suspension parameters, carbody loading statuses and the lengths of couplers. According to the parameters listed in Tab. 1, the calculated result of carbody-stabilizing-coupler stability is 410.97 kN. Literature[15] indicates that the distinct angling behaviour of coupler in DFC-E100 system is only observed when the longitudinal buff forces are larger than 460 kN. It also can be seen from Fig. 7 that the distinct angling behaviour of simulation model appears after the longitudinal forces reach 440.5 kN. Both the theoretical calculation result and simulation result of carbody-stabilizing-coupler ability have good agreement with the field test result.

Fig. 9 shows the time history of aligning torque of DFC-E100 system. Combined with Fig. 7, it can be seen that the aligning torque needed to stabilizing couplers increases with the longitudinal force. After the longitudinal force reaches it's maximum value, the aligning torque is dynamically stable at around 120 kN·m. Influenced by the stochastic vibration of carbody,

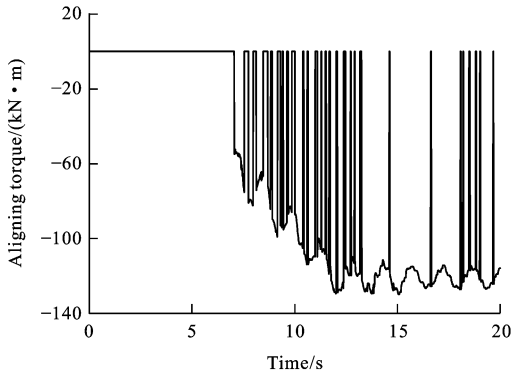

Fig. 9 Time history of aligning torque

coupler angle is not always in the maximum free angle state, so the time history of aligning torque presents a discrete state.

5.2 13A/QKX-100 system

Fig. 10 shows the dynamic behaviour of 13A/QKX-100 system bearing a longitudinal buff force. This figure demonstrates the obvious effect of friction pair, and no distinct coupler angling is recorded in simulation. Coupler angle fluctuates between 0.04° and −0.05°. Coupler force is also stabler than that of DFC-E100 system. All the phenomena agree with that of field test.

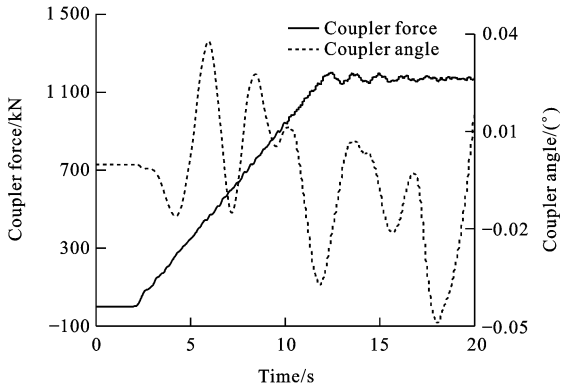

Fig. 10 Dynamic performances of 13A/QKX-100 system

Fig. 11 presents the time history of friction force at coupler tail of 13A coupler. Combined with Fig. 10, the friction force adaptively changes with coupler state, and the maximum friction force reaches 28.8 kN. The dynamic coupler stability is exact reason why coupler angle changes within a small range.

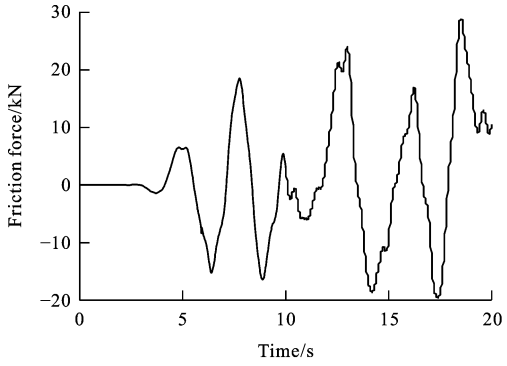

Fig. 11 Time history of friction force

6 Conclusions

Two nonlinear hysteresis draft gear models and two typical freight locomotive coupler system models are presented in this paper. The friction pair and real-time aligning shoulder models are integrated into the two systems respectively. The coupler systems are simulated in train models consisting of two 8-axle locomotives and one simplified wagon. The theoretical calculation of carbody-stabilizing-coupler ability is also performed. The results indicate that the models can rationally reflect the dynamic behaviours of coupler systems of freight locomotives. Coupler angling behaviour of DFC-E100 system is only observed after the longitudinal buff force reaches a certain level. Both the theoretical calculation result and simulation result of carbody-stabilizing-coupler ability have good agreement with field test result. Influenced by friction pair of 13A/QKX-100 system, no distinct coupler angling behaviour is detected when 13A coupler bears longitudinal buff force.

References:

[1] MA Wei-hua, SONG Rong-rong, JIE Chang-an, et al. Influences of buffer impedance characteristics on dynamics performances for heavy haul train[J]. Journal of Traffic and Transportation Engineering, 2011, 11(2): 59-64.

[2] YANG Jun-jie, LIU Jian-xin, LUO Shi-hui, et al. Test study on stability control of locomotive coupler in heavy haul combined train[J]. Journal of Southwest Jiaotong University, 2009, 44(6): 882-886.

[3] NCR, Datong Electric Locomotive Co., Ltd. The report on research & improvement of the HX_D2 coupler system[R]. Datong: NCR, Datong Electric Locomotive Co., Ltd., 2008.

[4] Transportation Safety Board of Canada. Railway investigation report R02C0050[R]. Ottawa: TSB Canada, 2002.

[5] CHERKASHIN U M, ZAKHAROV S M, SEMECHKIN A E. An overview of rolling stock and track monitoring systems and guidelines to provide safety of heavy and long train operation in the Russian railways[J]. Journal of Rail and Rapid Transit, 2009, 223(2): 199-208.

[6] NASR A, MOHAMMANDI S. The effects of train brake delay time on in-train forces[J]. Journal of Rail and Rapid Transit, 2010, 224(6): 523-534.

[7] CHANG Chong-yi, WANG Cheng-guo, MA Da-wei, et al. Study on numerical analysis of longitudinal forces of the T20 000 heavy haul[J]. Journal of the China Railway Society, 2006, 28(2): 89-94.

[8] EL-SIBAIE M. Recent advancements in buff and draft testing techniques[C]// ASME. Proceedings of 1993 IEEE/ASME Joint Railroad Conference. New York: ASME, 1993: 115-119.

(下转第 52 页)